

## Electronic Band Structure of $\text{BaCo}_2\text{As}_2$ : A Fully Doped Ferropnictide Analog with Reduced Electronic Correlations

N. Xu,<sup>1</sup> P. Richard,<sup>1,\*</sup> A. van Roekeghem,<sup>1,2</sup> P. Zhang,<sup>1</sup> H. Miao,<sup>1</sup> W.-L. Zhang,<sup>1</sup>  
T. Qian,<sup>1</sup> M. Ferrero,<sup>2</sup> A. S. Sefat,<sup>3</sup> S. Biermann,<sup>2,4</sup> and H. Ding<sup>1</sup>

<sup>1</sup>*Beijing National Laboratory for Condensed Matter Physics, and Institute of Physics,  
Chinese Academy of Sciences, Beijing 100190, China*

<sup>2</sup>*Centre de Physique Théorique, Ecole Polytechnique, CNRS-UMR7644, 91128 Palaiseau, France*

<sup>3</sup>*Materials Science and Technology Division, Oak Ridge National Laboratory, Oak Ridge, Tennessee 37831-6114, USA*

<sup>4</sup>*Japan Science and Technology Agency, CREST, Kawaguchi 332-0012, Japan*

(Received 18 October 2012; published 28 January 2013)

We report an investigation with angle-resolved photoemission spectroscopy of the Fermi surface and electronic band structure of  $\text{BaCo}_2\text{As}_2$ . Although its quasinesting-free Fermi surface differs drastically from that of its Fe-pnictide cousins, we show that the  $\text{BaCo}_2\text{As}_2$  system can be used as an approximation to the bare unoccupied band structure of the related  $\text{BaFe}_{2-x}\text{Co}_x\text{As}_2$  and  $\text{Ba}_{1-x}\text{K}_x\text{Fe}_2\text{As}_2$  compounds. However, our experimental results, in agreement with dynamical-mean-field-theory calculations, indicate that electronic correlations are much less important in  $\text{BaCo}_2\text{As}_2$  than in the ferropnictides. Our findings suggest that this effect is due to the increased filling of the electronic  $3d$  shell in the presence of significant Hund's exchange coupling.

DOI: [10.1103/PhysRevX.3.011006](https://doi.org/10.1103/PhysRevX.3.011006)

Subject Areas: Condensed Matter Physics, Strongly Correlated Materials, Superconductivity

Although the role they play in ferropnictide superconductivity is still not settled, there is sufficient evidence indicating that Fe-based superconductor systems exhibit non-negligible electronic correlations. Indeed, previous angle-resolved-photoemission-spectroscopy (ARPES) studies reported typical overall bandwidth renormalization of a factor of about 2–5 [1]. Interestingly, Hund's-rule coupling was identified as an efficient tuning parameter for electronic correlations [2–5], indicating the importance of local moments in the physics of these materials. Very recently [6], a study of hole-doped  $\text{BaFe}_2\text{As}_2$  evidenced an unusual non-Fermi-liquid behavior with frozen moments in the paramagnetic phase. The doping-temperature phase diagram of these materials exhibits exotic fractional power-law behavior of the many-body self-energies consistent with the phase diagram of the “spin-freezing” scenario [7], where fractional behaviors occur in some temperature range at fillings close to half-filling. (For a review, see Ref. [8].) Following this logic, one would expect the strength of the electronic correlations to vary significantly when the electronic structure is tuned away from the  $d^{6-x}$  filling of hole-doped  $\text{Ba}_{1-x}\text{K}_x\text{Fe}_2\text{As}_2$ , with reduced correlation effects when the  $d^7$  filling is reached.

An experimental characterization of the  $d^7$  filling state is thus called for.

In this work, we report ARPES results on  $\text{BaCo}_2\text{As}_2$  with a  $d^7$  filling. We determine its Fermi surface (FS) and electronic band structure by using polarized photons over a wide energy range. To quantify the strength of the electronic correlations, we compare the overall bandwidth found experimentally with the one predicted by our local-density-approximation (LDA) calculations, which ignore the electronic correlations. We find that the overall band structure is only 1.4 times narrower than predicted by our LDA calculations, indicating much weaker correlation effects than in its cousin  $\text{BaFe}_2\text{As}_2$ , for which a renormalization factor of 3 was reported [9]. We have performed dynamical-mean-field-theory (DMFT) calculations, which include the electronic correlations, and have found good agreement with the experimental ARPES spectra. Moreover, our results indicate that the weaker correlation effects in  $\text{BaCo}_2\text{As}_2$  as compared to those of the ferropnictides are mainly a consequence of the larger band filling in the Co compound. These findings support previous theoretical results by confirming the crucial role played by the Hund's-rule coupling in the ferropnictide materials [2–5]. In addition, they go beyond by allowing us to identify the filling of the  $d$  band as an efficient tuning parameter for the strength of electronic correlations in the larger family of ferro- and nonferropnictides in the presence of Hund's-rule coupling.

High-quality single crystals of  $\text{BaCo}_2\text{As}_2$  were grown by the flux method [10]. ARPES experiments were performed at beam lines PGM and Apple-PGM of the Synchrotron Radiation Center (Wisconsin) equipped with a Scienta

\*p.richard@iphy.ac.cn

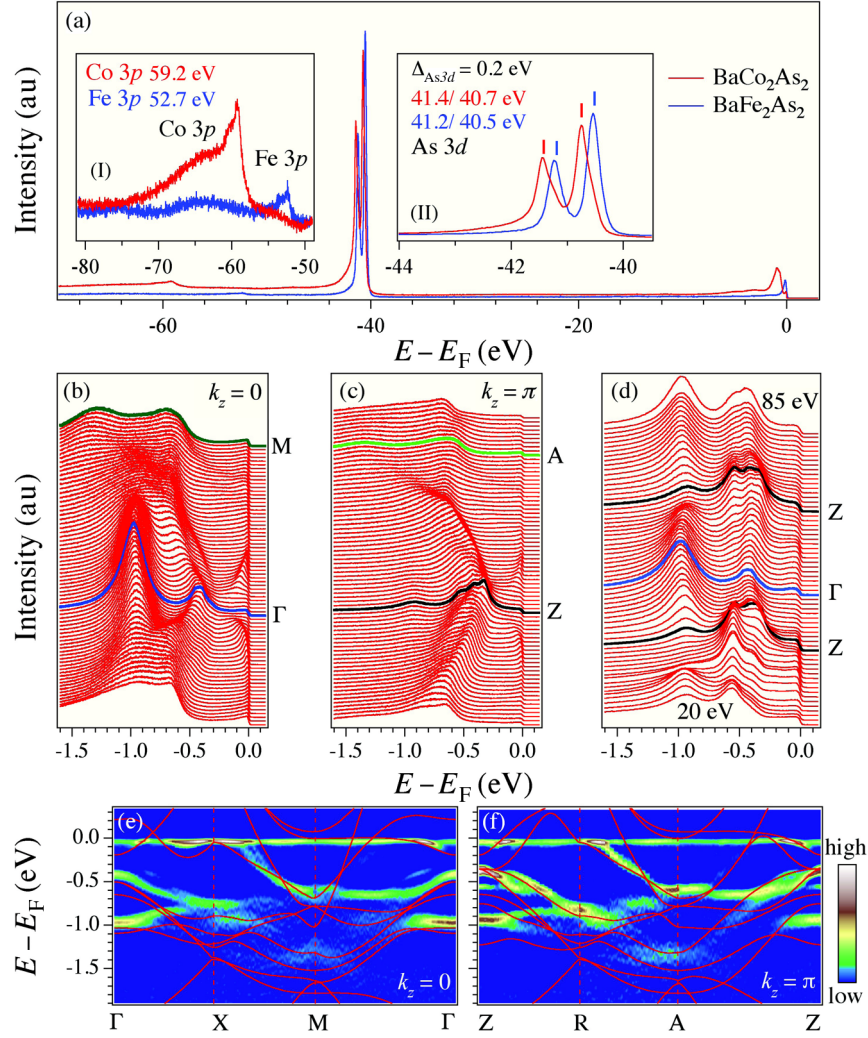


FIG. 1. (a) Core level spectra of  $\text{BaCo}_2\text{As}_2$  (red) and  $\text{BaFe}_2\text{As}_2$  (blue) recorded with 195-eV photons. Insets I and II are close-ups of the Fe (Co)  $3p$  and As  $4d$  levels, respectively. (b),(c) EDCs measured at 20 K along  $\Gamma$ -M ( $k_z = 0$ ) and Z-A ( $k_z = \pi$ ), respectively. (d) Photon-energy dependence of the EDCs taken at the BZ center. (e),(f) 2D curvature-intensity plots [17] along high-symmetry lines in the  $k_z = 0$  and  $k_z = \pi$  planes, respectively. Nonrenormalized LDA bands are overlapped for comparison.

SES 200 analyzer and a Scienta R4000 analyzer, respectively. The energy and angular resolutions were set at 15–30 meV and  $0.2^\circ$ , respectively. The samples were cleaved *in situ* and measured at 20 K in a vacuum better than  $5 \times 10^{-11}$  Torr. We label the momentum values with respect to the 1 Fe/unit-cell Brillouin zone (BZ), and use  $c' = c/2$  as the distance between two Fe planes. The DMFT calculations were performed using the TRIQS toolkit [11] and its implementation of the hybridization expansion continuous-time quantum Monte Carlo algorithm [12,13], using Legendre polynomials [14].

Wide-energy photoemission spectra of  $\text{BaCo}_2\text{As}_2$  (red) and  $\text{BaFe}_2\text{As}_2$  (blue) are compared in Fig. 1(a). A well-defined Co  $3p$  core level observed at 59.2 eV below the Fermi energy ( $E_F$ ) in the  $\text{BaCo}_2\text{As}_2$  spectrum (inset I), in contrast to 52.7 eV for the Fe  $3p$  core level in  $\text{BaFe}_2\text{As}_2$ , confirms the sample compositions. As expected from a previous ARPES study [15] and confirmed by band-

structure calculations [16], this different composition is accompanied by an upward shift of the chemical potential. Consequently, the As  $3d$  core levels (inset II) are observed to shift by 200 meV toward higher binding energy in  $\text{BaCo}_2\text{As}_2$  as compared with  $\text{BaFe}_2\text{As}_2$ . We note that the As  $3d$  peaks have asymmetric profiles, which is consistent with the enhanced coherence of the  $\text{BaCo}_2\text{As}_2$  valence electrons.

To fully investigate the dispersive states near  $E_F$ , we performed ARPES experiments over a wide photon-energy range. We show energy distribution curves (EDCs) recorded along the  $\Gamma(0, 0, 0)$ -M( $\pi, 0, 0$ ) and Z( $0, 0, \pi$ )-A( $\pi, 0, \pi$ ) directions in Figs. 1(b) and 1(c), respectively. The two sets of data are different, suggesting a strong 3D character of the electronic structure emphasized by the photon-energy dependence of the EDC spectrum at the BZ center displayed in Fig. 1(d). At first sight, the results are quite different from those of previous studies on the

122 ferropnictides [1]. In particular, an electron band (rather than hole bands) crosses  $E_F$  around the  $\Gamma$  point. This is indeed what is expected from our LDA calculations, which are shown in Figs. 1(e) and 1(f). Actually, an overall band renormalization of only 1.4 is needed to capture the essential dispersive features highlighted in the curvature-intensity plots [17] also shown in Figs. 1(e) and 1(f) for high-symmetry directions. In contrast, the electronic correlations in Ba<sub>0.6</sub>K<sub>0.4</sub>Fe<sub>2</sub>As<sub>2</sub> place the compound at the boundary of an exotic non-Fermi-liquid state, where

coherent quasiparticles are ill-defined quantities. To fit spectral features to a renormalized LDA band structure requires renormalization of at least a factor of 2 [18]. We attribute this decrease in the strength of the electronic correlations to the less drastic effects of Hund's-rule coupling [19] in the  $d^7$  compound BaCo<sub>2</sub>As<sub>2</sub> as compared to the  $d^{6-x}$  filling of the  $d$  shell in hole-doped BaFe<sub>2</sub>As<sub>2</sub>. We will come back to this point below.

Photoemission selection rules give further information on the nature of the electronic bands observed.

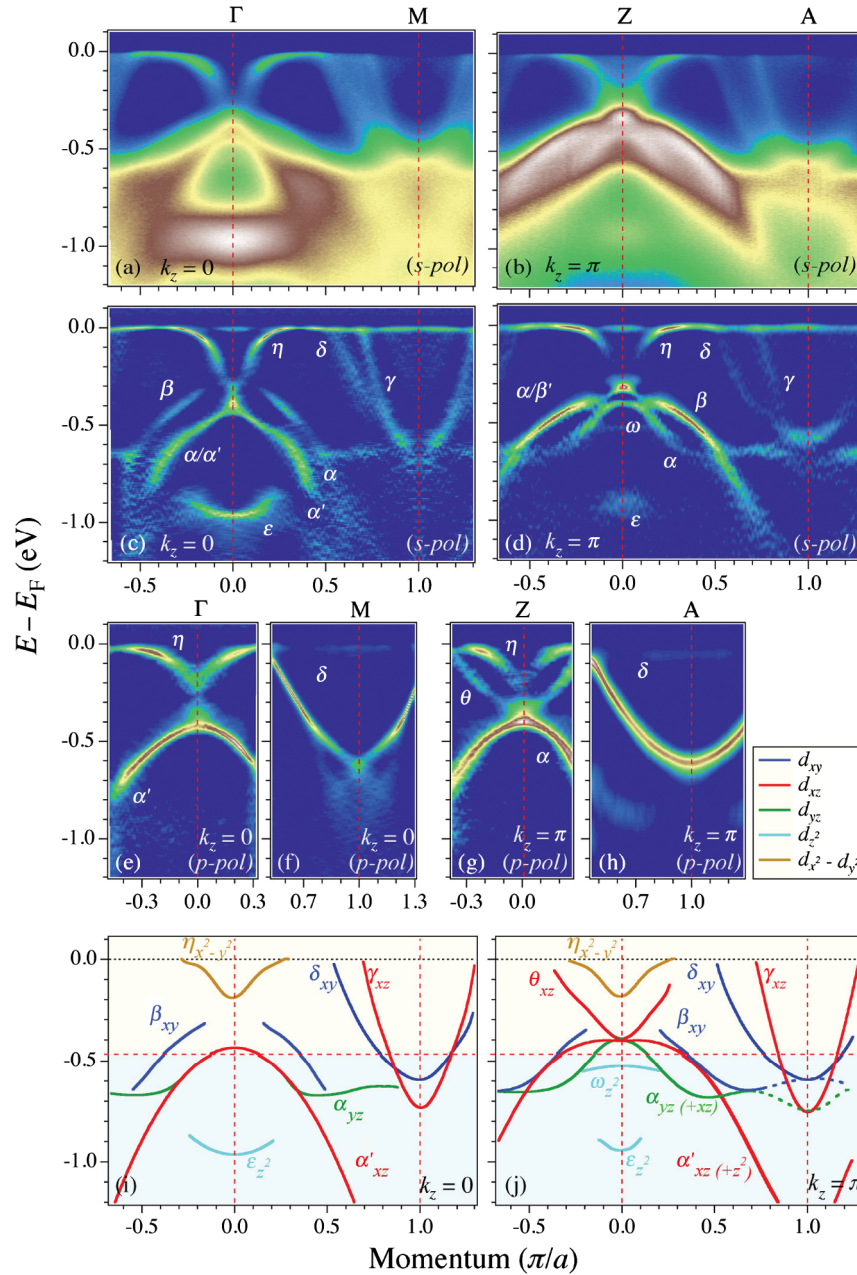


FIG. 2. (a),(b) ARPES intensity plots of BaCo<sub>2</sub>As<sub>2</sub> along  $\Gamma$ -M and Z-A, respectively, recorded in the  $s$  polarization ( $s$ - $pol$ ) geometry. (c),(d) Corresponding 2D curvature-intensity plots [17]. (e)–(h) 2D curvature-intensity plots for data recorded with  $p$  polarization ( $p$ - $pol$ ) around (e)  $\Gamma$ , (f) M, (g) Z, and (h) A. (i)–(j) Band dispersions extracted from MDC fits along  $\Gamma$ -M and Z-A, respectively, along with their orbital characters determined from LDA calculations and the polarization data.

In Figs. 2(a) and 2(b), we show the ARPES intensity plots corresponding to data recorded with an  $s$  polarization (with a polarization component along the  $z$  axis) along the  $\Gamma$ -M and Z-A high-symmetry lines, respectively. For a better visualization of the dispersion band, we also plot the corresponding curvature-intensity plots in Figs. 2(c) and 2(d). Similarly, the data recorded with a  $p$  polarization are displayed in Figs. 2(e) and 2(f) for the  $k_z = 0$  plane and in Figs. 2(g) and 2(h) for the  $k_z = \pi$  plane. While the  $s$  polarization enhances bands with odd symmetries with respect to the photoemission plane, the  $p$  polarization highlights mainly the even symmetries. Two bands,  $\delta$  and  $\gamma$ , cross  $E_F$  at the M (A) point, independent of  $k_z$ . While both appear clearly with  $s$  polarization, only the  $\delta$  band is detected with  $p$  polarization, suggesting that the other one, the  $\gamma$  band, has an odd character. Similarly, two electron bands, called  $\eta$  and  $\theta$ , cross  $E_F$  at the BZ center. The first one is detected at  $\Gamma$  and Z but appears stronger under  $s$  polarization, suggesting an odd character. The effect of the polarization is more severe on the  $\theta$  band, which is observed only around the Z point under  $p$  polarization. Since the folding potential on the Fe site due to As

atoms cannot be neglected [20,21], we have projected the various orbital characters on our LDA-calculated bands in order to facilitate the assignment of the orbital character of each band. Based on our measurements and in comparison with our LDA calculations, we can determine the orbital characters of all bands forming the FS, as well as all the bands down to a binding energy of 1.4 eV. The results are summarized in Figs. 2(i) and 2(j) for the  $k_z = 0$  and  $k_z = \pi$  planes, respectively.

In Figs. 3(a) and 3(b), we display our LDA calculations for the FS cuts at  $k_z = 0$  and  $k_z = \pi$ , respectively. The corresponding ARPES data, obtained by integrating the ARPES intensity within  $E_F \pm 10$  meV, are shown in Figs. 3(d) and 3(e), respectively. As expected from the previous analysis of the band structure in the vicinity of  $E_F$ , the FS topology of  $\text{BaCo}_2\text{As}_2$  is quite different from that of the Fe pnictides. For example, the more or less circular hole FS pockets at the  $\Gamma$  point of superconducting  $\text{Ba}_{0.6}\text{K}_{0.4}\text{Fe}_2\text{As}_2$  [18] are replaced by star-shaped electron FS pockets in  $\text{BaCo}_2\text{As}_2$ , thus removing all possibility for electron-hole quasineesting scattering in this system. In Fig. 3(f), we show the  $k_z$  dispersion at  $E_F$  approximated

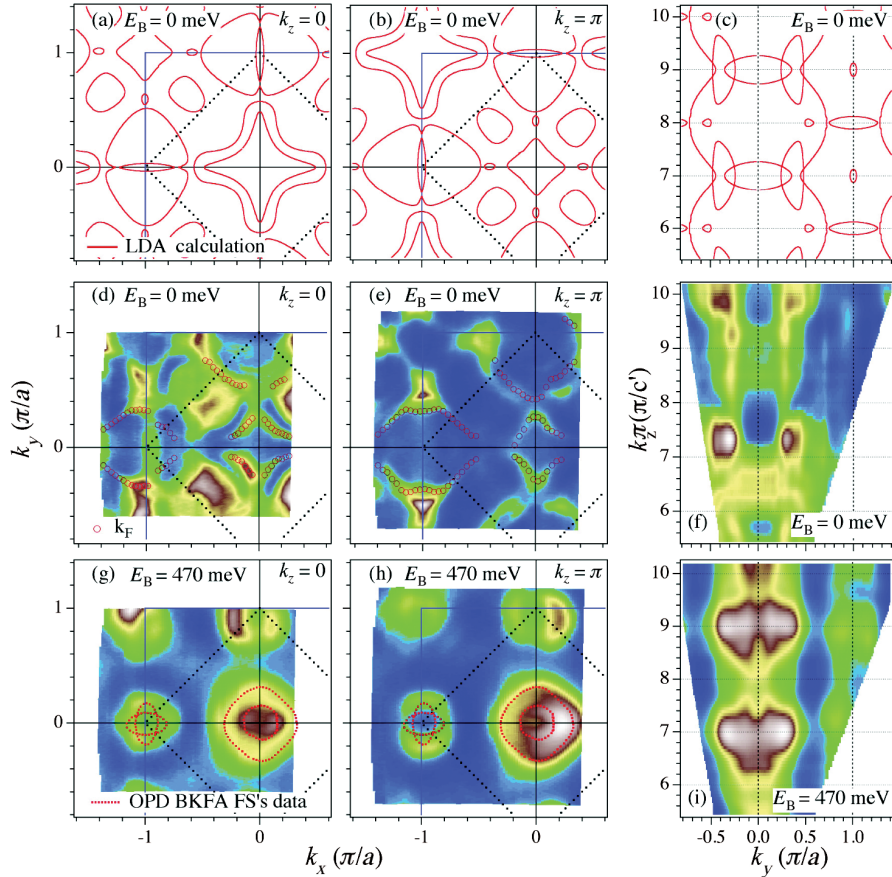


FIG. 3. (a),(b) LDA cuts of the FS at  $k_z = 0$  and  $k_z = \pi$ , respectively. (c) LDA FS in the plane defined by  $k_y = 0$ . (d)–(f) Experimental FS mappings corresponding to the cases described in panels (a)–(c). The open symbols represent extracted FS data. (g)–(i) Same as (d)–(f) but for ARPES data recorded 470 meV below  $E_F$ . The ARPES FS data [18] for  $\text{Ba}_{0.6}\text{K}_{0.4}\text{Fe}_2\text{As}_2$  (red dashed lines) are plotted in (g),(h) for comparison.

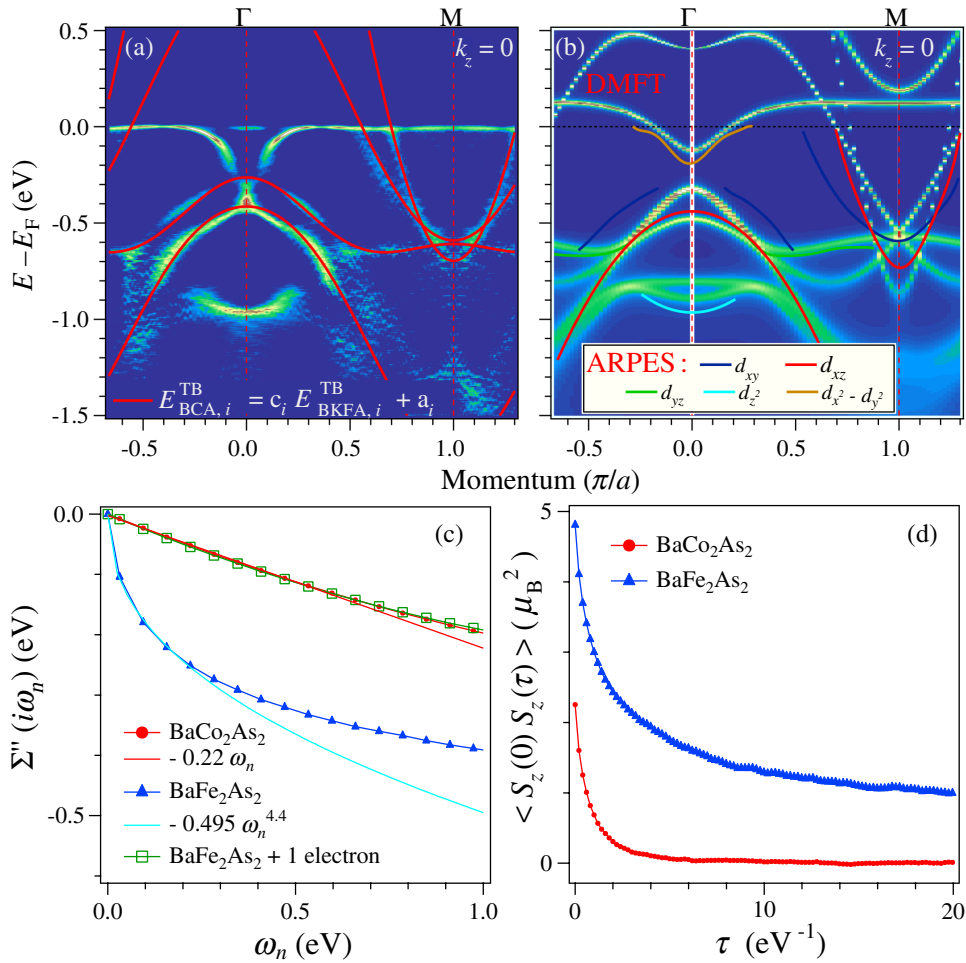


FIG. 4. (a) 2D curvature-intensity plot [17] along  $\Gamma$ -M compared with a tight-binding-band fit (red lines). A direct correspondence between the tight-binding energy  $E_{\text{BCA},i}^{\text{TB}}$  of the  $i$ th band in BaCo<sub>2</sub>As<sub>2</sub> and the tight-binding energy  $E_{\text{BKFA},i}^{\text{TB}}$  of the  $i$ th band in Ba<sub>1-x</sub>K<sub>x</sub>Fe<sub>2</sub>As<sub>2</sub> is obtained after multiplying the latter band by a factor  $c_i$  and shifting it by a constant  $a_i$ . Except for a 470-meV rigid band shift, the bandwidth of the  $\beta$  band is 4 times larger than in Ba<sub>0.6</sub>K<sub>0.4</sub>Fe<sub>2</sub>As<sub>2</sub> [18], in contrast to 2 times for all other bands. (b) LDA + DMFT calculation of the band structure of BaCo<sub>2</sub>As<sub>2</sub> (120 K). The experimental bands are overlapped for comparison. (c) Imaginary part of the self-energy (120 K) as a function of the Matsubara frequency for BaCo<sub>2</sub>As<sub>2</sub>, BaFe<sub>2</sub>As<sub>2</sub>, and the hypothetical compound consisting of BaFe<sub>2</sub>As<sub>2</sub> with one additional electron per Fe atom. While a linear fit is performed for the BaCo<sub>2</sub>As<sub>2</sub> data, the BaFe<sub>2</sub>As<sub>2</sub> data are fit with a power-law  $A\omega_n^\alpha$ , for which we found  $\alpha = 0.44$ . (d) DMFT calculation of the spin-spin correlations in BaCo<sub>2</sub>As<sub>2</sub> and BaFe<sub>2</sub>As<sub>2</sub> at 120 K.

by scanning the photon energy over a wide range, and we display the corresponding LDA calculation in Fig. 3(c). We note that the  $\eta$  and  $\delta$  bands have a strong 2D character, which is consistent with our assignment of their orbital character. On the other hand, the  $\gamma$  band exhibits a small warping that could be caused by a small hybridization with the  $p_z$  orbital according to our LDA calculations.

Although the FS of BaCo<sub>2</sub>As<sub>2</sub> differs substantially from that of the 122 ferropnictides, we find that the constant energy maps recorded at 470 meV below  $E_F$  for the  $k_z = 0$  and  $k_z = \pi$  planes, which are, respectively, displayed in Figs. 3(g) and 3(h), are quite similar to the FSs of Ba<sub>0.6</sub>K<sub>0.4</sub>Fe<sub>2</sub>As<sub>2</sub>. To illustrate this resemblance, we overlap on these figures the FSs obtained for Ba<sub>0.6</sub>K<sub>0.4</sub>Fe<sub>2</sub>As<sub>2</sub> in Ref. [18]. In a similar fashion, the  $k_x k_z$  map at 470 meV

binding energy displayed in Fig. 3(i) could easily be mistaken for the  $k_z$  dispersion at  $E_F$  of some typical 122 ferropnictides [22,23].

At least qualitatively, the simplest explanation for this behavior is to assume an approximately 470-meV upward shift of the chemical potential following a 3d-shell filling from  $3d^6$  in BaFe<sub>2</sub>As<sub>2</sub> to  $3d^7$  in BaCo<sub>2</sub>As<sub>2</sub>. As shown in Figs. 2(g) and 2(h), all the bands in BaCo<sub>2</sub>As<sub>2</sub> below a binding energy of 470 meV find their near- $E_F$  equivalent in the 122 ferropnictides with the same orbital assignment [24]. At the  $\Gamma$  point, for example, the  $\alpha$  and  $\alpha'$  bands are degenerate over a wide momentum range at  $k_z = 0$ , whereas, at  $k_z = \pi$ , they merge only at the Z point. Their relative position with respect to the  $\beta$  band is also the same as in Ba<sub>0.6</sub>K<sub>0.4</sub>Fe<sub>2</sub>As<sub>2</sub> [24]. For a more quantitative

comparison, we use for the  $k_z = 0$  data a tight-binding band model [25] that has been successfully applied previously to  $\text{Ba}_{0.6}\text{K}_{0.4}\text{Fe}_2\text{As}_2$  [18]:

$$E^{\alpha,\beta}(k_x, k_y) = E_0^{\alpha,\beta} + t_1^{\alpha,\beta}(\cos k_x + \cos k_y) + t_2^{\alpha,\beta} \cos k_x \cos k_y, \quad (1)$$

$$E^{\gamma,\delta}(k_x, k_y) = E_0^{\gamma,\delta} + t_1^{\gamma,\delta}(\cos k_x + \cos k_y) + t_2^{\gamma,\delta} \cos(k_x/2) \cos(k_y/2). \quad (2)$$

The results of the fit are overlapped in Fig. 4(a) with the curvature-intensity plot at  $k_z = 0$ . The agreement with the data is quite good. Disregarding a 470-meV shift for the chemical potential, we find that all the fit parameters, except  $t_1^\beta$  and  $t_2^\beta$  which are 4 times larger, are twice as large as the parameters obtained for  $\text{Ba}_{0.6}\text{K}_{0.4}\text{Fe}_2\text{As}_2$  [18]. Our experimental data suggest that  $\text{BaCo}_2\text{As}_2$  can be viewed in a first rough approximation as a highly overdoped and nonmagnetically ordered  $\text{BaFe}_2\text{As}_2$  compound, thus allowing us to visualize the unoccupied states in the superconducting 122 ferropnictides. More important though, our data indicate clearly that  $\text{BaCo}_2\text{As}_2$  is less correlated than  $\text{Ba}_{0.6}\text{K}_{0.4}\text{Fe}_2\text{As}_2$ .

As observed in  $\text{Ba}(\text{Fe}_{1-x}\text{Ru}_x)_2\text{As}_2$  [23,26], a large decrease in the electronic correlations is expected as  $3d$  electrons are substituted by  $4d$  electrons. The situation is quite different in  $\text{Ba}(\text{Fe}_{1-x}\text{Co}_x)_2\text{As}_2$ , where the conducting properties of both  $\text{Fe}^{2+}$  and  $\text{Co}^{2+}$  derive from  $3d$  electron orbitals with similar spatial extension. To investigate the nature of this unexpected decrease of the electronic correlations in  $\text{BaCo}_2\text{As}_2$ , we have performed LDA + DMFT calculations on this material and on paramagnetic  $\text{BaFe}_2\text{As}_2$  using the experimental crystal parameters. The corresponding results are shown in Fig. 4(b). The technical details of the calculations are analogous to what was described in Ref. [27], supplementing the LDA Hamiltonian by explicit local Coulomb-interaction terms of density-density form. The Coulomb-interaction matrix is parametrized using the standard representation in terms of the Slater integrals  $F_0, F_2, F_4$ , which are calculated within the constrained random phase approximation in the implementation of Ref. [28]. The results we present in Fig. 4(c) for  $\text{BaCo}_2\text{As}_2$  show a remarkable agreement with the experimental data. We extract a quasiparticle weight  $Z$  of 0.8 leading to a mass enhancement of 1.25 that compares well to the experiment. We find a power-law behavior of the self-energy in  $\text{BaFe}_2\text{As}_2$  for calculations at the same temperature (120 K), signaling the absence of coherent quasiparticles. However, the corresponding spectral functions are consistent with an apparent renormalization of the low-energy LDA bands by a factor of 2.9, in agreement with the factor 3 observed experimentally [9].

In Fig. 4(c), we plot the imaginary part of the self-energy  $\Sigma''(i\omega_n)$  of both  $\text{BaCo}_2\text{As}_2$  and paramagnetic  $\text{BaFe}_2\text{As}_2$  as a function of the Matsubara frequencies.

While  $\Sigma''(i\omega_n)$  varies linearly at low frequency in  $\text{BaCo}_2\text{As}_2$ , indicating coherent Fermi-liquid behavior already at the temperature of the calculation ( $T = 120$  K), it follows a nearly square-root behavior characteristic of the “spin-freezing” regime in  $\text{BaFe}_2\text{As}_2$ . To investigate further the origin of this phenomenon, we have artificially added 1 electron per Fe in  $\text{BaFe}_2\text{As}_2$  to mimic the effect of substitution, while maintaining the LDA Hamiltonian of this compound. Surprisingly, the self-energy of this hypothetical crystal can hardly be distinguished from that of  $\text{BaCo}_2\text{As}_2$ , as shown in Fig. 4(c). This result strongly suggests that the decrease in the electronic correlations in  $\text{BaCo}_2\text{As}_2$  is mainly due to the less drastic effects of Hund’s exchange in the Co compound whose  $d^7$  filling is further away from the case of a half-filled shell. An analogous effect has recently been studied in a three-orbital Hubbard model [7], where Hund’s exchange was found to induce an exotic “spin-freezing” regime at finite temperatures for incommensurate fillings close to the half-filled case. This explanation rules out any significant influence from structural variations [29]. Indeed, this huge change in the level of correlations cannot be linked to a variation of the Coulomb parameter  $U$ . In both cases, we find  $U = F_0$  around 2.8–2.9 and the Hund’s coupling  $J_H = (F_2 + F_4)/14$  around 0.85, with even a small increase of  $U$  in the Co case. Furthermore, we have performed additional calculations in which we artificially set  $J_H$  to 0. In this case, we see a sudden drop of the renormalization and the suppression of the non-Fermi-liquid behavior in  $\text{BaFe}_2\text{As}_2$ . However,  $\text{BaCo}_2\text{As}_2$  becomes only slightly less correlated. The fact that the spin-freezing scenario is realized at fillings close (but not equal) to half-filling is consistent with the unified view of the pnictide and cuprate superconductors put forward *e.g.*, in Refs. [5,30], where the proximity to Mottness, that is, to the  $d^5$  filling of the Mott insulator, is considered as the decisive parameter to tune electronic correlations. Indeed, also in the pnictide family,  $d^5$  compounds (such as  $\text{LaMnPO}$  [31] or  $\text{BaMn}_2\text{As}_2$  [32]) have been synthesized and characterized as good insulators. Our findings demonstrate that the evolution—as a function of filling—of the  $d^5$  manganite insulators into the strongly correlated and badly metallic  $d^6$  ferropnictides can be further extended into a weakly correlated regime for the higher fillings of the  $d$  shell in the cobaltates.

Early experimental results suggested the presence of large unscreened local moments in some ferropnictide materials [33]. Our results emphasize further the importance of these moments. In the spin-freezing regime, these unscreened local moments have a long lifetime, and spin-spin correlation functions do not decay anymore [7]. As shown by our DMFT calculations of the spin-spin correlations plotted in Fig. 4(d), this situation corresponds to  $\text{BaFe}_2\text{As}_2$  at the temperature of the calculations. In contrast, the spin-spin correlations in  $\text{BaCo}_2\text{As}_2$  decay rapidly and become vanishingly small in the long-time limit.

The apparent strength of the electronic correlations increases with the local moments. Thus, correlations in the ferropnictides can be interpreted as the interaction of local moments with itinerant electrons, as in the Kondo problem. In the present study, we have compared two compounds with small orbital polarization (due to the strength of Hund's coupling): BaFe<sub>2</sub>As<sub>2</sub>, with six electrons in five bands, and BaCo<sub>2</sub>As<sub>2</sub>, with seven electrons in five bands. In the former case, Hund's exchange drastically reduces the available channels for Kondo screening, thus enhancing the consequences of electronic correlations, while in the latter, screening is quite efficient and reestablishes a largely uncorrelated picture. We stress that this effect is not primarily due to the density of states. Indeed, a calculation with five degenerate bands gives qualitatively the same conclusion, and the reduction of orbital polarization by Hund's coupling is likely to push the compound close to that model case.

In summary, we have used ARPES to characterize the electronic band structure of BaCo<sub>2</sub>As<sub>2</sub>. We have shown that this material can be used as a first approximation to investigate the unoccupied states of the 122 ferropnictides. However, supported by LDA + DMFT calculations, our study indicates that BaCo<sub>2</sub>As<sub>2</sub> is significantly less correlated than BaFe<sub>2</sub>As<sub>2</sub> at equal Hund's-rule coupling, due to the larger filling of the *d* electron shell. Our results reveal clearly the importance of local moments in the physics of the Fe-based superconductors and establish the *d*-shell filling as the most important tuning parameter for electronic correlations in the series of Mn, Fe, or Co pnictides.

We acknowledge X. Dai, Z. Fang, Z. Wang, and J.-P. Hu for useful discussions, as well as O. Parcollet for help with the numerical calculations. This work was supported by grants from CAS (No. 2010Y1JB6), MOST (Nos. 2010CB923000 and 2011CBA001000), NSFC (11004232 and 11050110422), computing time at IDRIS/GENCI (under Project No. 1193), the Cai Yuanpei program, and the French ANR (project PNICTIDES). This work is based in part on research conducted at the Synchrotron Radiation Center, which is primarily funded by the University of Wisconsin-Madison with supplemental support from facility Users and the University of Wisconsin-Milwaukee. This research was partially supported by the U.S. Department of Energy, Basic Energy Sciences, Materials Sciences and Engineering Division.

- 
- [1] P. Richard, T. Sato, K. Nakayama, T. Takahashi, and H. Ding, *Fe-Based Superconductors: An Angle-Resolved Photoemission Spectroscopy Perspective*, *Rep. Prog. Phys.* **74**, 124512 (2011).
- [2] K. Haule and G. Kotliar, *Coherence-Incoherence Crossover in the Normal State of Iron Oxyprictides and Importance of Hund's Rule Coupling*, *New J. Phys.* **11**, 025021 (2009).

- [3] M. Aichhorn, S. Biermann, T. Miyake, A. Georges, and M. Imada, *Theoretical Evidence for Strong Correlations and Incoherent Metallic State in FeSe*, *Phys. Rev. B* **82**, 064504 (2010).
- [4] A. Liebsch and H. Ishida, *Correlation-Induced Spin Freezing Transition in FeSe: A Dynamical Mean Field Study*, *Phys. Rev. B* **82**, 155106 (2010).
- [5] H. Ishida and A. Liebsch, *Fermi-Liquid, Non-Fermi-Liquid, and Mott Phases in Iron Pnictides and Cuprates*, *Phys. Rev. B* **81**, 054513 (2010).
- [6] P. Werner, M. Casula, T. Miyake, F. Aryasetiawan, A. J. Millis, and S. Biermann, *Satellites and Large Doping and Temperature Dependence of Electronic Properties in Hole-Doped BaFe<sub>2</sub>As<sub>2</sub>*, *Nat. Phys.* **8**, 331 (2012).
- [7] P. Werner, E. Gull, M. Troyer, and A. J. Millis, *Spin Freezing Transition and Non-Fermi-Liquid Self-Energy in a Three-Orbital Model*, *Phys. Rev. Lett.* **101**, 166405 (2008).
- [8] A. Georges, L. de' Medici, and J. Mravlje, *Strong Electronic Correlations from Hund's Coupling*, [arXiv:1207.3033](https://arxiv.org/abs/1207.3033).
- [9] P. Richard, K. Nakayama, T. Sato, M. Neupane, Y.-M. Xu, J. H. Bowen, G. F. Chen, J. L. Luo, N. L. Wang, X. Dai, Z. Fang, H. Ding, and T. Takahashi, *Observation of Dirac Cone Electronic Dispersion in BaFe<sub>2</sub>As<sub>2</sub>*, *Phys. Rev. Lett.* **104**, 137001 (2010).
- [10] A. S. Sefat, D. J. Singh, R. Jin, M. A. McGuire, B. C. Sales, and D. Mandrus, *Renormalized Behavior and Proximity of BaCo<sub>2</sub>As<sub>2</sub> to a Magnetic Quantum Critical Point*, *Phys. Rev. B* **79**, 024512 (2009).
- [11] Michel Ferrero and Olivier Parcollet, *Continuous-Time Solver for Quantum Impurity Models TRIQS: A Toolbox for Research on Interacting Quantum Systems*, <http://ipht.cea.fr/triqs>.
- [12] Philipp Werner, Armin Comanac, Luca De' Medici, Matthias Troyer, and Andrew J. Millis, *Continuous-Time Solver for Quantum Impurity Models*, *Phys. Rev. Lett.* **97**, 076405 (2006).
- [13] Emanuel Gull, Andrew J. Millis, Alexander I. Lichtenstein, Alexey N. Rubtsov, Matthias Troyer, and Philipp Werner, *Continuous-Time Monte Carlo Methods for Quantum Impurity Models*, *Rev. Mod. Phys.* **83**, 349 (2011).
- [14] Lewin Boehnke, Hartmut Hafermann, Michel Ferrero, Frank Lechermann, and Olivier Parcollet, *Orthogonal Polynomial Representation of Imaginary-Time Green's Functions*, *Phys. Rev. B* **84**, 075145 (2011).
- [15] M. Neupane, P. Richard, Y.-M. Xu, K. Nakayama, T. Sato, T. Takahashi, A. V. Federov, G. Xu, X. Dai, Z. Fang, Z. Wang, G.-F. Chen, N.-L. Wang, H.-H. Wen, and H. Ding, *Electron-Hole Asymmetry in the Superconductivity of Doped BaFe<sub>2</sub>As<sub>2</sub> Seen via the Rigid Chemical-Potential Shift in Photoemission*, *Phys. Rev. B* **83**, 094522 (2011).
- [16] T. Berlijn, C.-H. Lin, W. Garber, and W. Ku, *Do Transition-Metal Substitutions Dope Carriers in Iron-Based Superconductors?*, *Phys. Rev. Lett.* **108**, 207003 (2012).
- [17] P. Zhang, P. Richard, T. Qian, Y.-M. Xu, X. Dai, and H. Ding, *A Precise Method for Visualizing Dispersive Features in Image Plots*, *Rev. Sci. Instrum.* **82**, 043712 (2011).

- [18] H. Ding, K. Nakayama, P. Richard, S. Souma, T. Sato, T. Takahashi, M. Neupane, Y.-M. Xu, Z.-H. Pan, A. V. Fedorov, Z. Wang, X. Dai, Z. Fang, G. F. Chen, J. L. Luo, and N. L. Wang, *Electronic Structure of Optimally Doped Pnictide Ba<sub>0.6</sub>K<sub>0.4</sub>Fe<sub>2</sub>As<sub>2</sub>: A Comprehensive Angle-Resolved Photoemission Spectroscopy Investigation*, *J. Phys. Condens. Matter* **23**, 135701 (2011).
- [19] L. de' Medici, J. Mravlje, and A. Georges, *Janus-Faced Influence of Hund's Rule Coupling in Strongly Correlated Materials*, *Phys. Rev. Lett.* **107**, 256401 (2011).
- [20] Chia-Hui Lin, Tom Berlijn, Limin Wang, Chi-Cheng Lee, Wei-Guo Yin, and Wei Ku, *One-Fe versus Two-Fe Brillouin Zone of Fe-Based Superconductors: Creation of the Electron Pockets by Translational Symmetry Breaking*, *Phys. Rev. Lett.* **107**, 257001 (2011).
- [21] V. Brouet, M. F. Jensen, Ping-Hui Lin, A. Taleb-Ibrahimi, P. Le Fèvre, F. Bertran, Chia-Hui Lin, Wei Ku, A. Forget, and D. Colson, *Impact of the Two Fe Unit Cell on the Electronic Structure Measured by ARPES in Iron Pnictides*, *Phys. Rev. B* **86**, 075123 (2012).
- [22] W. Malaeb, T. Yoshida, A. Fujimori, M. Kubota, K. Ono, K. Kihou, P.M. Shirage, H. Kito, A. Iyo, H. Eisaki, Y. Nakajima, T. Tamegai, and R. Arita, *Three-Dimensional Electronic Structure of Superconducting Iron Pnictides Observed by Angle-Resolved Photoemission Spectroscopy*, *J. Phys. Soc. Jpn.* **78**, 123706 (2009).
- [23] N. Xu, T. Qian, P. Richard, Y.-B. Shi, X.-P. Wang, P. Zhang, Y.-B. Huang, Y.-M. Xu, H. Miao, G. Xu, G.-F. Xuan, W.-H. Jiao, Z.-A. Xu, G.-H. Cao, and H. Ding, *Effects of Ru Substitution on Electron Correlations and Fermi-Surface Dimensionality in Ba(Fe<sub>1-x</sub>Ru<sub>x</sub>)<sub>2</sub>As<sub>2</sub>*, *Phys. Rev. B* **86**, 064505 (2012).
- [24] X.-P. Wang, P. Richard, Y.-B. Huang, H. Miao, L. Cevey, N. Xu, Y.-J. Sun, T. Qian, Y.-M. Xu, M. Shi, J.-P. Hu, X. Dai, and H. Ding, *Orbital Characters Determined from Fermi Surface Intensity Patterns Using Angle-Resolved Photoemission Spectroscopy*, *Phys. Rev. B* **85**, 214518 (2012).
- [25] M.M. Korshunov and I. Eremin, *Theory of Magnetic Excitations in Iron-Based Layered Superconductors*, *Phys. Rev. B* **78**, 140509(R) (2008).
- [26] V. Brouet, F. Rullier-Albenque, M. Marsi, B. Mansart, M. Aichhorn, S. Biermann, J. Faure, L. Perfetti, A. Taleb-Ibrahimi, P. Le Fèvre, F. Bertran, A. Forget, and D. Colson, *Significant Reduction of Electronic Correlations upon Isovalent Ru Substitution of BaFe<sub>2</sub>As<sub>2</sub>*, *Phys. Rev. Lett.* **105**, 087001 (2010).
- [27] M. Aichhorn, L. Pourovskii, V. Vildosola, M. Ferrero, O. Parcollet, T. Miyake, A. Georges, and S. Biermann, *Dynamical Mean-Field Theory within an Augmented Plane-Wave Framework: Assessing Electronic Correlations in the Iron Pnictide LaFeAsO*, *Phys. Rev. B* **80**, 085101 (2009).
- [28] L. Vaugier, Hong Jiang, and Silke Biermann, *Hubbard U and Hund Exchange J in Transition Metal Oxides: Screening versus Localization Trends from Constrained Random Phase Approximation*, *Phys. Rev. B* **86**, 165105 (2012).
- [29] We caution though that structural variations are actually important around a doping level of 6 electrons, especially near the crossover between Fermi liquid and non-Fermi liquid. For instance, trying to hole-dope the BaCo<sub>2</sub>As<sub>2</sub> compound gives a very different picture, with a finite part of  $\Sigma''(0)$ , indicating that this compound is pushed even further into the spin-freezing phase.
- [30] T. Misawa, K. Nakamura, and M. Imada, *Ab Initio Evidence for Strong Correlation Associated with Mott Proximity in Iron-Based Superconductors*, *Phys. Rev. Lett.* **108**, 177007 (2012).
- [31] J. W. Simonson, Z. P. Yin, M. Pezzoli, J. Guo, J. Liu, K. Post, A. Efimenko, N. Hollmann, Z. Hu, H.-J. Lin, C.-T. Chen, C. Marques, V. Leyva, G. Smith, J. W. Lynn, L. L. Sun, G. Kotliar, D. N. Basov, L. H. Tjeng, and M. C. Aronson, *From Antiferromagnetic Insulator to Correlated Metal in Pressurized and Doped LaMnPO*, *Proc. Natl. Acad. Sci. U.S.A.* **109**, E1815 (2012).
- [32] A. T. Satya, A. Mani, A. Arulraj, N. V. Chandra Shekar, K. Vinod, C. S. Sundar, and A. Bharathi, *Pressure-Induced Metallization of BaMn<sub>2</sub>As<sub>2</sub>*, *Phys. Rev. B* **84**, 180515(R) (2011).
- [33] F. Bondino, E. Magnano, M. Malvestuto, F. Parmigiani, M. A. McGuire, A. S. Sefat, B. C. Sales, R. Jin, D. Mandrus, E. W. Plummer, D. J. Singh, and N. Mannella, *Evidence for Strong Itinerant Spin Fluctuations in the Normal State of CeFeAsO<sub>0.89</sub>F<sub>0.11</sub> Iron Oxypnictide Superconductors*, *Phys. Rev. Lett.* **101**, 267001 (2008).